

See discussions, stats, and author profiles for this publication at: <https://www.researchgate.net/publication/262114484>

Development of New Antiatherosclerotic and Antithrombotic Drugs Utilizing F11 Receptor (F11R/JAM-A) Peptides

Article in *Peptide Science* · July 2014

DOI: 10.1002/bjp.22503

CITATIONS

0

READS

146

8 authors, including:



Anna Babinska

State University of New York Downstate Medical Center

49 PUBLICATIONS 614 CITATIONS

[SEE PROFILE](#)



Cristina Clement

Albert Einstein College of Medicine

109 PUBLICATIONS 2,179 CITATIONS

[SEE PROFILE](#)



Maria Swiatkowska

Medical University of Łódź

39 PUBLICATIONS 564 CITATIONS

[SEE PROFILE](#)



Jacek Szymanski

Medical University of Łódź

28 PUBLICATIONS 282 CITATIONS

[SEE PROFILE](#)

Some of the authors of this publication are also working on these related projects:



F11R/JAM-A and Atherosclerosis [View project](#)



MOMENTO [View project](#)

Development of New Antiatherosclerotic and Antithrombotic Drugs Utilizing F11 Receptor (F11R/JAM-A) Peptides

A. Babinska,^{1,2} C. C. Clement,³ M. Swiatkowska,⁴ J. Szymanski,⁴ A. Shon,¹ Y. H. Ehrlich,⁵ E. Kornecki,^{1,2} M. O. Salifu¹

¹Division of Nephrology, Department of Medicine, State University of New York, Downstate Medical Center, Brooklyn, NY 11203

²Department of Cell Biology and Medicine, State University of New York, Downstate Medical Center, Brooklyn, NY 11203

³Department of Chemistry, Lehman College of the City University of New York Bronx, NY 10468

⁴Department of Molecular and Medical Biophysics, Medical University of Lodz, 92-215, Lodz, Poland

⁵Program in Neuroscience, College of Staten Island of the City University of New York, Staten Island, NY 10314

Received 14 January 2014; revised 1 April 2014; accepted 2 May 2014

Published online 7 May 2014 in Wiley Online Library (wileyonlinelibrary.com). DOI 10.1002/bip.22503

ABSTRACT:

Peptides with enhanced resistance to proteolysis, based on the amino acid sequence of the F11 receptor molecule (F11R, aka JAM-A/Junctional adhesion molecule-A), were designed, prepared, and examined as potential candidates for the development of anti-atherosclerotic and anti-thrombotic therapeutic drugs. A sequence at the N-terminal of F11R together with another sequence located in the first Ig-loop of this protein, were identified to form a steric active-site operating in the F11R-dependent adhesion between cells that express F11R molecules on their external surface. In silico modeling of the complex between two polypeptide chains with the sequences positioned in the active-site was used to generate peptide-candidates designed to inhibit homophilic interactions between surface-located F11R molecules. The two lead F11R peptides were modified with D-Arg and D-Lys at selective sites, for attaining higher stability to proteolysis in vivo. Using molecular docking experiments we tested

different conformational states and the putative binding affinity between two selected D-Arg and D-Lys-modified F11R peptides and the proposed binding pocket. The inhibitory effects of the F11R peptide ${}^2\text{HN}-(\text{dK})\text{-SVT}-(\text{dR})\text{-EDTGTYTC-CONH}_2$ on antibody-induced platelet aggregation and on the adhesion of platelets to cytokine-inflamed endothelial cells are reported in detail, and the results point out the significant potential utilization of F11R peptides for the prevention and treatment of atherosclerotic plaques and associated thrombotic events.

© 2014 Wiley Periodicals, Inc. *Biopolymers (Pept Sci)* 102: 322–334, 2014.

Keywords: peptide 4D; F11 receptor; F11R/JAMA; anti-atherosclerotic drug; antithrombotic drug

This article was originally published online as an accepted preprint. The “Published Online” date corresponds to the preprint version. You can request a copy of the preprint by emailing the Biopolymers editorial office at biopolymers@wiley.com

INTRODUCTION

F11R is the name of the gene for the constitutively expressed platelet membrane adhesion protein, termed the F11 receptor¹ (aka Junctional adhesion molecule, JAM-A). The NIH-Nomenclature Committee assigned for the human F11R protein the gene

Additional Supporting Information may be found in the online version of this article.

Correspondence to: Dr. Anna Babinska, SUNY Downstate Medical Center, Medicine 450 Clarkson Av, Box#52, Brooklyn, New York; e-mail: ababinska@downstate.edu

© 2014 Wiley Periodicals, Inc.

number AF207907, and the number BC021876 for the murine molecule F11r. The F11R protein was identified, characterized, and purified^{1,2} using a specific platelet-stimulatory, anti-F11R, monoclonal antibody (termed M.Ab.F11) that induced platelet aggregation upon its addition to human platelet suspensions. The cloning of F11R,³ followed by the characterization of the genomic structure and the organization of the F11R gene, along with the analysis of its promoter region⁴ revealed multiple regulatory sites associated with involvement in inflammatory thrombosis. In the healthy physiological state of the vasculature, the F11R molecule is constitutively expressed on the surface of circulating platelets and within tight junctions of endothelial cells (EC),¹⁻⁴ being absent on the luminal surface of the EC. In the healthy endothelium, the F11R is localized within its tight junctions^{5,6} thereby preventing the otherwise pathological adherence of platelets to the vasculature. Several reports^{7,8} have provided evidence that under pathophysiological conditions, platelets do adhere to the endothelium, a process which further initiates atherosclerotic plaque formation, leading to systemic atherosclerosis and inflammatory thrombosis. Our previous studies have provided evidence demonstrating that F11R is a major adhesion molecules involved in platelet interactions with the vessel wall under inflammatory conditions, and that the action of F11R is critical for the adhesion of platelets to inflamed EC.^{9,10} Furthermore, significant over-expression of F11R molecules has been found in the vasculature of atherosclerotic-prone animals, as well as in major vessels of clinically diagnosed, human coronary artery disease patients,¹² indicating the pathophysiological link of F11R to cardiovascular disorders.

Based on the data generated by our basic research we hypothesized that the initial adhesion of platelets to an inflamed vessel wall is mediated by F11R, initiating plaque formation and atherogenesis, then leading to the development of atherosclerosis. In order to test this hypothesis and examine experimentally the pathological interactions mediated by F11R, we have first identified the amino acid sequences within the active, adhesion site of this protein. Two such sequences were identified, Peptide 1 in the N-terminus and peptide 4 in the first Ig fold of the F11R molecule. Both are part of the protein-protein recognition interface. The physiological potential of these peptides could be validated as inhibitors of key platelet activities: the aggregation of platelets and the adhesion of platelets to cytokine-inflamed EC. The crystal structure of F11R¹¹ shows that the sequences of peptides 1 [SVTVHSSEPEVRIPENNPVKLSC] and 4 [KSVTREDTGYTC] are located adjacent to one-another on the protein surface, suggesting that the identified peptides may inhibit the homodimeric F11R interactions by mimicking and binding to these sites.^{11,12} Subsequent

studies from our group have identified F11R as an important molecule in inflammatory thrombosis and atherosclerosis, highlighting the platelets as critical factors involved in the progression and development of cardiovascular disease.^{13,14,16}

In the study reported here we describe a structure-based design-approach aimed at improving the potency and stability to proteolysis of the originally identified lead F11R-inhibitory peptides. Using molecular docking experiments we tested different conformational states and the putative binding affinity between two selected D-Arg and D-Lys-modified F11R peptides and the proposed binding pocket between the surface-exposed F11R adhesion molecules of platelets and inflamed EC.¹⁶ The replacement of L-Arg and L-Lys isomers with their corresponding D-isomers at selective sites within the peptides 1 and 4 was expected to render peptides of greater stability to proteolysis in vivo. The D-Arg and D-Lys peptides were further tested for their ability to block two pathophysiological activities: agonist-induced platelet aggregation and the adhesion of platelets to cytokine-inflamed endothelial cells. The new lead peptide 4D [₂HN-(dK)-SVT-(dR)-EDTGYTC-CONH₂] emerged as a candidate for clinical utilization in the prevention and/or causing regression, namely treatment, of atherosclerotic plaques and linked thrombotic events.

MATERIALS AND METHODS

Design of F11R Peptides 1D and 4D With Enhanced Resistance to Proteolysis

In our previous studies, two F11R peptides (termed peptides 1 and 4) were proven to display inhibitory activities in functional assays involving platelet aggregation and adhesion, whereas another F11R peptide (termed peptide 5 with the amino acid sequence of EQDGSP-PSEYTWFKD) was shown to be non-inhibitory in these assays.¹⁶ The amino acid sequences of peptide 1 - SVTVHSSEPEVRIPENNPVKLSC and peptide 4 - KSVTREDTGYTC were used to design and synthesize two D-amino acid analogs, named peptides 1D and 4D, respectively, for greater stability to protease digestion by thrombin and trypsin, when administered in vivo. The amino acid sequence of the analog peptides 1D - SSEPEV-dR-IPENNPV and 4D - dKSVT-dR-EDTGYTC provides information on the location of the D-amino acid substitutions. The peptides were predicted to be digested by many proteases using the "PeptideCutter" website at ExPASy server (http://web.expasy.org/peptide_cutter/). As shown in the Supporting Information Table 1, we generated numerous D-analogs corresponding to each amino acid involved in the cleavage sites predicted for each protease. We present in this article only the analogs expected to be resistant to hydrolysis primarily by thrombin and/or trypsin, because of the involvement and accumulation of active thrombin at sites of atherosclerotic plaques, as reported¹³ thus increasing the life-time duration of analogs at these sites. Increased resistance of D-peptide analogs to trypsin hydrolysis would be expected to enhance their life-time in blood, where trypsin-like proteases are involved in the homeostasis of coagulation and fibrinolysis.

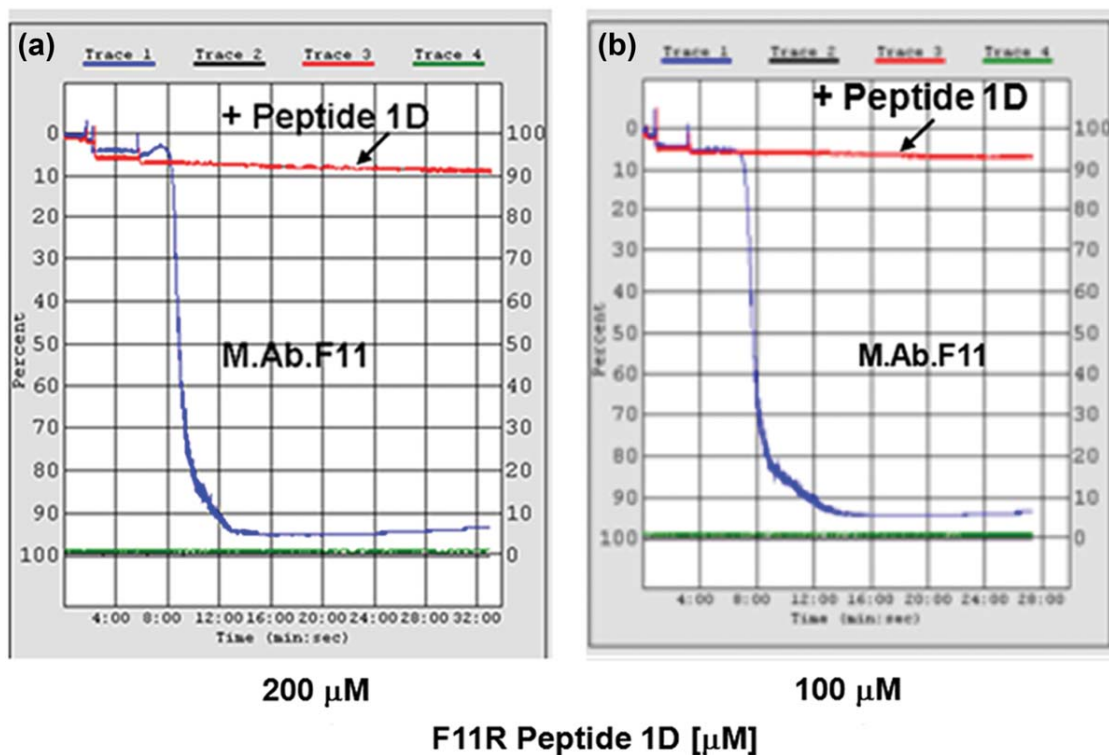


FIGURE 1 Inhibition of human platelet aggregation by hydrolysis-resistant F11R-peptide 1D. Panels a and b show the complete inhibition of agonist M.Ab.F11-induced human platelet aggregation in the presence (red tracings) of either 200 or 100 μM peptide 1D, respectively. Blue tracings in each panel depict the full-blown platelet aggregation induced by M.Ab.F11 that resulted in the presence of a control, irrelevant, scrambled peptide. The arrows indicate aggregation tracings obtained in the presence of peptide 1D. Each tracing is representative of tracings obtained in three separate experiments.

Synthesis and Purification of F11R Peptides

Peptides were synthesized using standard solid phase fluorenylmethyloxycarbonyl (Fmoc) chemistry on a 432A Synergy Personal Peptide synthesizer (ABI) as previously described.¹⁴ Briefly, amide Rink resin (Novabiochem) was used to produce all peptides as C-terminal amides. The peptides were cleaved from the resin and side-chain-protecting groups removed after treatment for 3–4 h with a cleavage cocktail consisting of 50 μL of ethanedithiol, 5 μL of thioanisole, and 900 μL trifluoroacetic acid (TFA) and precipitated with cold methyl tert-butyl ether. Peptides were solubilized in 50% (v/v) acetonitrile. The filtered crude material was then purified on a C18 reversed-phase column (Phenomenex) using a linear gradient of 0–75% acetonitrile in 0.1% TFA, at a rate of 2% per minute. The identity of each peptide was determined by electrospray ionization (ESI) mass spectrometry run in the positive mode.

F11R 4D-Analog Peptide Resistance to Proteolysis

The analog peptide 4D (20 μM) was incubated with alpha-thrombin and trypsin (20 nM) at room temperature in phosphate buffer pH 7.46 (pH 8.0 for trypsin) with 0.2 M NaCl and 5mM CaCl_2 . An independent experiment was conducted with the

peptide analog 4-L. After 24 h incubation, aliquots were removed and the reactions were quenched with 0.1% TFA. The samples were analyzed on an ESI spectrometer run in the positive mode. The spectra were acquired between 100 and 2000 m/z. The predicted average mass of peptide 4-D/L is 1460.5 (based on the amino acid sequence, using the ProtParameter tools at the ExPasy server (<http://web.expasy.org/protparam/>)). The peptide would have an m/z of 1461.5 if charged 1+ (+1H⁺) or 730.25 if charged 2+ (+2H⁺).

Platelet Aggregation

Human platelets were washed and isolated from fresh, whole blood as described previously.¹¹ Platelet aggregation experiments were carried-out in a Chronolog Lumi-Aggregometer (Chronolog Corp., Haverton, PA), and initiated by the addition of aliquots of the anti-F11R monoclonal antibody, M.Ab.F11, to isolated platelet suspensions ($2\text{--}4 \times 10^8$ platelets/mL). The two major parameters characterizing platelet aggregation, i.e., the extent of platelet aggregation, expressed in light transmission units (LTU) and the initial velocity of aggregation (LTU/min), were quantitatively recorded for each set of assay conditions.

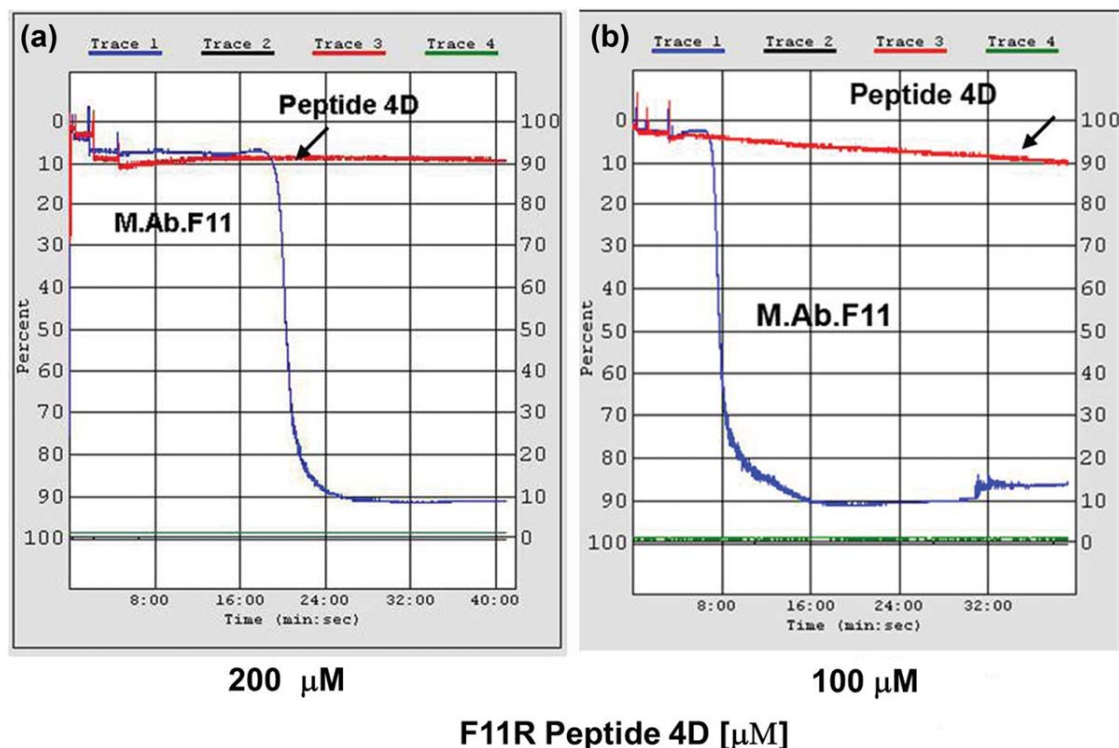


FIGURE 2 Inhibition of M.Ab.F11-induced platelet aggregation by hydrolysis-resistant F11R peptide 4D. Panels a and b: Inhibition of M.Ab.F11-induced aggregation by the presence of 200 and 100 μM peptide 4D, respectively (tracings in red color). Controls: Full-blown platelet aggregations, induced by M.Ab.F11 in the present of a scrambled peptide, are depicted by the blue-colored tracings in each panel. The arrows point to the aggregation tracings obtained in the presence of peptide 4D. Each tracing is representative of tracings obtained in three separate experiments.

Binding Assays for the F11R L-and D-Analog Peptides

Two types of solid-phase binding assays were used in this study: the first involved the immobilization of M.Ab.F11 onto microtiter plates, while the second type of assay involved the immobilization of the F11R recombinant protein.

- A solid-phase binding assay containing immobilized M.Ab.F11 was utilized for testing the inhibitory effects of F11R peptides on the binding of F11R protein to M.Ab.F11. Microtiter wells (Maxisorp; Nunc, Roskilde, Denmark) were coated with 10 $\mu\text{g}/\text{mL}$ of either M.Ab.F11 (BD PharmingenTM, San Jose, CA) or BSA (control). The binding of the soluble, biotinylated recombinant F11R (JAM-A/Fc-biotin (Invitrogen, Eugene, OR) to the immobilized M.Ab.F11 was performed in binding buffer (Tris-buffered saline, TBS, pH 7.4, 0.5% BSA, 1 mM Mg^{++} , 1 mM Ca^{++}). The inhibition of specific binding was performed in the presence of the increasing concentrations of the following

compounds, with incubation carried-out for 1 h at 37°C: F11R (JAM-A/Fc (R&D systems, Minneapolis, MN), F11R peptide 4, nonhydrolyzable F11R peptide (peptide F11R 4D), or a noninhibitory F11R peptide (F11R peptide 5 with amino acid sequence EQDGSP-PSEYTWFKD) used here as a negative control. The total amount of biotinylated F11R bound was detected with peroxidase-conjugated streptavidin, quantified using the substrate reagent kit (R&D Systems).

- The second solid phase binding assay contained the immobilized F11R protein for quantifying the homophilic interaction between soluble F11R and the bound F11R protein. Microtiter wells (Maxisorp; Nunc, Roskilde, Denmark) were coated with 25 $\mu\text{g}/\text{mL}$ F11R (JAM-A/Fc, R&D systems, Minneapolis, MN) or BSA (10 $\mu\text{g}/\text{mL}$) in 10 mM Tris, pH 9. Binding of biotinylated F11R (JAM-A/Fc- biotin purchased from Invitrogen, Eugene OR) to immobilized F11R was performed in binding buffer (TBS), 0.5% BSA, 1 mM Mg^{++} ,

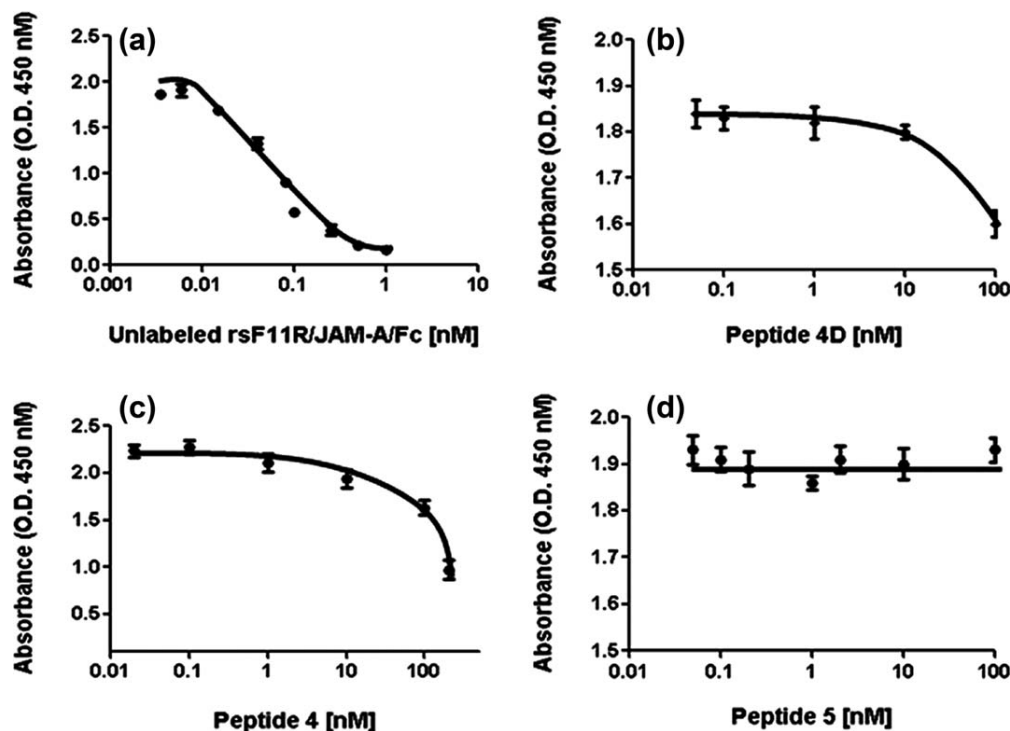


FIGURE 3 F11R peptide 4D inhibits the binding of biotin-labeled F11R to immobilized M.Ab.F11: Solid phase binding assay. Inhibition of the specific binding of biotinylated F11R (F11R/JAM-A/Fc-biotin) to immobilized MAbF11 by the presence of the following: (Panel a), unlabeled recombinant F11R (aka recombinant soluble JAM-A, rsJAM-A/Fc); (Panel b), F11R Peptide 4D; (Panel c), F11R Peptide 4 (original sequence); (Panel d), Peptide 5, control peptide. The value of the fraction of bound ligand is given as mean \pm SD of three separate experiments. A nonlinear regression model was used to fit the experimental data.

1 mM Ca^{++}) containing increasing concentrations of unlabeled F11R, peptide 4 or nonhydrolyzable peptide 4D, incubated for 1 h at 37°C. After washings with 0.05% Tween/TBS, the specifically bound F11R-biotin was detected with peroxidase-conjugated streptavidin and quantified using the substrate reagent kit (R&D Systems).

Monitoring of the Role of F11R in the Adhesion of Platelets to the Inflamed Endothelium

To quantitate the number of viable platelets bound to cytokine-inflamed EC, human platelets were labeled using calcein AM, as previously described.^{14–16} Briefly, the platelet-rich plasma (PRP) was prepared from 100 mL of citrated whole blood, by centrifugation at 200g for 20 min at 23°C. Calcein AM (2 $\mu\text{g}/\text{mL}$) (Invitrogen) was added to the PRP, and the PRP was maintained at 30°C for 1 h in the absence of light. Platelets were isolated from PRP, washed as detailed¹ and resuspended at final concentrations ranging from 2.5 to 3.5 $\times 10^8/\text{mL}$. Assays conducted for measuring the adhesion of platelets to human aortic endothelial cells (HAEC) and human umbilical vein

endothelial cells (HUVEC) were performed in the dark. Initially, HAEC and HUVEC, plated in cell culture wells, were incubated with 1% FBS/BSA in 200M media for 1 h at 37°C to block nonspecific binding sites. Aliquots of freshly prepared, calcein-labeled platelets ($3.3 \times 10^8/\text{mL}$) were added to each of the cell-culture wells, and plates were incubated at 37°C for 1 h. Paraformaldehyde(4%), pH 7.4, was added to each well and incubation continued at 23°C for 15 min. The addition of paraformaldehyde, before washings, did not affect the natural capacity of the platelets to adhere to endothelial cells. The plates were washed 3 \times with prewarmed growth factor-free 200M media. Then aliquots (100 μL) of prewarmed PBS were added to wells, and wells were read using a Perkin Elmer plate reader Victor 3, 1420 multilabel counter with fluorescein filter, as previously described.^{14,19,20}

Incubation of EC With Peptide F11R 4D and the Administration of Proinflammatory Cytokines to EC

D-analog peptide 4D, dissolved in H_2O (10 mM), was diluted in culture media (0.5, 1 mM) prior to each test. The HAEC and HUVEC were grown to confluence and incubated with peptide 4D (in culture media without growth factor supplements) for 1 h at 37°C.

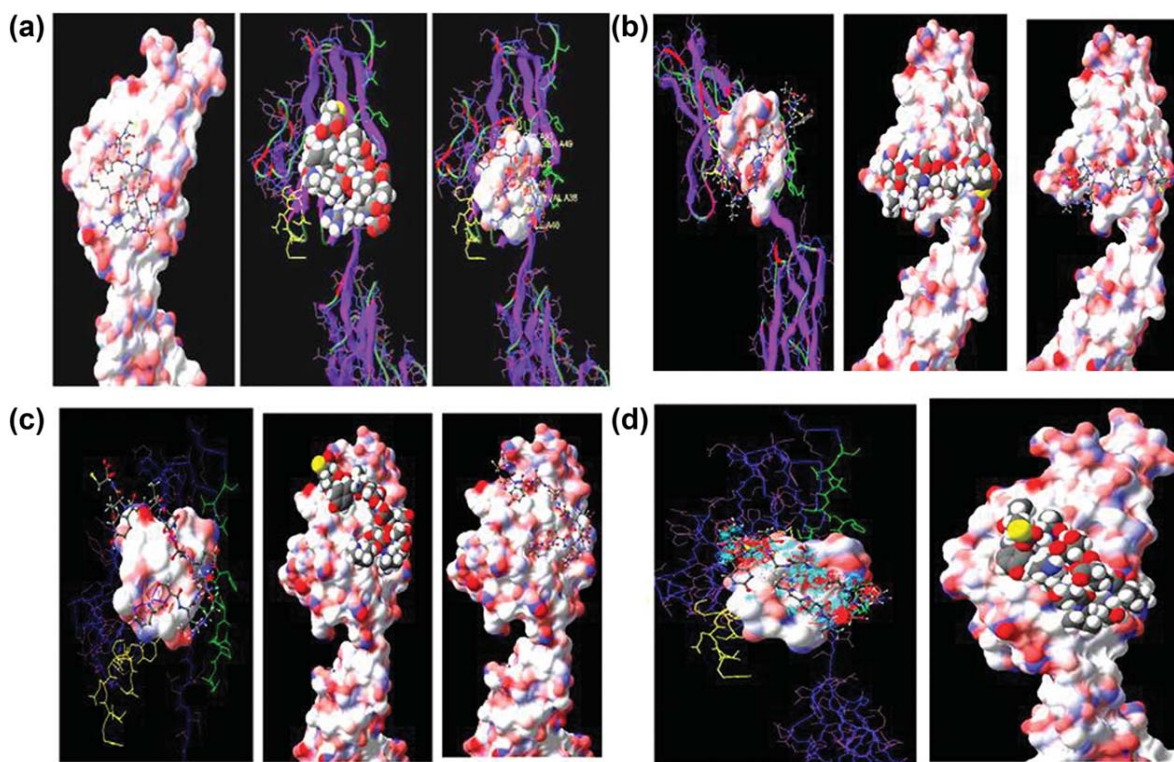


FIGURE 4 Docking of peptide 4D within the binding pocket of the F11R molecule (aka JAM-1, chain A, 1nbq.pdb). The docking software “Sculpt” was used to generate conformations of peptide 4D within regions predicted to be the steric active site of F11R.¹⁶ Molecular visualization of peptide bound to putative binding pocket of F11R was performed with the built-in package in the SCULPTs environment. The peptide is depicted as “balls and sticks” (Figures 4a–4c, left and right panels, and Figure 4d, left panel); or as “Van der Waals spheres-space filling” molecular models (Figures 4a–4c, center panels, and Figure 4d, right panel) using the standard CPK color code (red for “oxygen,” blue for “nitrogen,” gray for “carbon,” white for “hydrogen” and yellow for “sulfur”). The molecular model using the Van der Waals surface area (vdWSA) was used to represent the whole protein (color code; red for acidic, blue for basic, and white for hydrophobic/neutral environment) (Figure 4a, left panel; Figures 4b, 4c, middle and right panels; and Figure 4d, right panel). In addition, the secondary structure elements of the protein are shown as “purple” for beta strands and barrels, “red” for the turns and “green” for the protein loops (Figure 4a, middle and right panels and Figure 4b, left panel). In some models, the protein is shown as sticks (including the amino acids side chains) (Figures 4c, 4d left panels). As representative model for the interactive docking procedure allowed by the SCULPT environment, we choose to show the “favorable” (colored blue) and the “unfavorable” (colored red) shells of interaction between the ligand peptide 4D, and the putative pocket in F11R (Figure 4d left panel). This combination of different molecular models used to highlight the peptide binding to the protein receptor pocket allowed to delineate the structural and chemical requirements for achieving the molecular complementarity of this complex interaction between the peptide and the binding pocket of F11R. Each conformation was characterized by a relative binding energy of interaction (in kcal/mol) determined from both the van der Waals and a combination of van der Waals and electrostatic interactions. The major amino acids contributing to the binding interface are shown for each conformation. (Panel a) Conformation - 1: Energy of interaction: -138.6 kcal/mol (van der Waals); -556 kcal/mol (van der Waals and electrostatics). Binding pocket consists of: Val38, Ile40, Asn44, Pro45, Val46, Lys47, Ser49, Gly93, Thr95. (Panel b) Conformation - 2: -145.7 kcal/mol (van der Waals); -591.6 kcal/mol (van der Waals and electrostatics) Binding pocket consists of: Ser82, Tyr83, Asp85, Arg86, Val87, Phe96, Lys97, Ser98, Val99, Thr100, Ar101, Glu102, Asp103. (Panel c) Conformation - 3: -151.7 kcal/mol (van der Waals); -593.6 kcal/mol (van der Waals and electrostatics). Binding pocket consists of: Lys47, Cys50, Tyr52, Val60, Asn77, Thr88, Phe89, Leu90, Pro91, Thr92, Gly93, Ile94, Thr95 (Panel d) Conformation - 4: -142.2 kcal/mol (van der waals); -531.8 kcal/mol (van der Waals and electrostatics). Binding pocket consists of: Ser34, Glu35, Val38, Ile40, Asn44, Pro45, Val46, Lys47, Leu48, Ser49, Gly93, Thr95.

Afterwards, the proinflammatory cytokines, TNF α and/or IFN γ were added and the cultures were further incubated at 37°C for up to 24 h.

Homophilic Interactions Between Peptide 4D and the Recombinant Mouse F11r Protein Using the BIAcore X

Real time biomolecular interaction analysis was performed by surface plasmon resonance technology, using a BIAcore X apparatus equipped with a Sensor Chip CM-5 (BIAcore AB). Proteins were covalently attached to the surface of a CM5 sensor using amine coupling chemistry (BIAcore AB amine coupling kit) according to the manufacturer's instructions. The range of SPR signals after binding of the recombinant human protein (rhF11R) and the recombinant murine protein (rmF11r) to the sensor chip were on a similar level (1900–2100 RU). A sensor chip with immobilized BSA (2000 RU) was used as a control for assessing binding specificity. Experiments were performed at 25°C with the use of HBS as a running buffer (pH 7.4) with a flow rate of 10 μ L/min. Sensorgrams were analyzed with BIAevaluation 3.1 software (BIAcore AB).

The association and dissociation constants were determined by global fitting of the data using the Langmuir binding model (one-to-one interaction). The dissociation constant (K_D) was obtained by calculating the ratio of the dissociation (k_d) and association (k_a) rate constants (k_d/k_a), the association constant K_A was determined as $1/K_D$.

Molecular Docking and In Silico Structure-Based Design of Lead Peptide Inhibitors of F11R Homophilic Interaction

The new lead compounds derived from the original peptide 4 were docked into the protein template for F11R (aka F11R/JAM-1/JAM-A chain A, PDB entry 1nbq.pdb.¹⁸ The new peptide structures were drawn with ISIS Draw 2.2.1 (Accelrys), imported as 3D-structures in SCULPT (Accelrys), and manually docked into the proposed binding pocket between the surface-exposed F11R adhesion molecules of platelets and inflamed EC.¹⁶ The resulting F11R peptide complex was minimized using the SCULPT built-in molecular mechanics force field (MMFF94). After each round of minimization of the complex between F11R and the peptide ligand, the free energy of interaction (scoring function) was assessed using both Van der Waals and electrostatic force fields. In all docking experiments, the protein was “frozen” while the peptide was “thawed” using the corresponding functions from the SCULPT software. This procedure ensured the flexible conformational search for the peptide ligand into the active site of target protein and limited the conformational states of the protein template itself.¹⁵

RESULTS

The F11R peptide analogs, peptides 1D and 4D, containing D-arg and D-lys at selective positions, with enhanced resistance to proteolysis by trypsin and thrombin, were synthesized and examined for their effects on platelet function. The enhanced resistance of D-peptide analogs to proteolysis by thrombin was an essential requirement, as the enhanced activity exhibited by thrombin at sites of atherosclerotic plaque formation has been shown to result in an increased atherothrombosis and rupture

of plaques.¹⁷ To generate peptide analogs with enhanced lifetime at atherosclerotic sites, we explored the main cleavage sites for thrombin in both peptides 1 and 4D analogs and performed evaluations of their stability to thrombin digestion. In addition, we tested their stability to trypsin which was predicted to cleave both peptide analogs at selected positions, the C-term of R and K within the peptide sequence (Supporting Information Table 1). The in vitro proteolysis assay conducted in the presence of thrombin and trypsin for both the 4L and D-peptide analogs showed that peptide 4D was not hydrolyzed by thrombin and was more stable to hydrolysis by trypsin as compared with the 4L peptide (Supporting Information Figure 1).

As shown in Figures 1 and 2 (Panel a), complete inhibition of M.Ab.F11-induced platelet aggregation occurred in the presence of 200 μ M of either peptide 1D or 4D. Similarly, Figures 1 and 2 (Panel b) show that both peptides 1D and 4D, at a concentration of 100 μ M, strongly inhibited platelet aggregation induced by M.Ab.F11. We found that the inhibition of platelet aggregation using lower concentrations of peptides, was too variable between blood-donors to be quantified with reliability.

Because of the close homology of the amino acid sequence of the human F11R peptide 4 to the homologous murine F11r sequence, together with findings that we could attain complete inhibition of platelet aggregation by peptide 4D, peptide 4D was selected as the prime focus for the continuation of these studies. Utilizing peptide 4D, further experiments were performed to measure its potential inhibitory effects in biological assays, as presented in Figure 3. In solid phase binding assays, measuring the interactions between soluble and immobilized proteins, we compared the inhibitory potencies of recombinant F11R (panel a), the original peptide 4 (panel c), and the nonhydrolyzable peptide 4D (panel b). An IC_{50} value of 0.13 nM was measured for the soluble recombinant F11R protein for blockade of the binding of biotin-labeled F11R to the immobilized M.Ab.F11. In contrast to the blockade observed with nanomolar concentrations of the soluble recombinant F11R protein, higher concentrations (10- to 100-fold) of peptides 4L and 4D, of 10–100 nM, were required for such inhibition. The specificity of peptide 4D in such blockade can be seen by comparing its potency to that of the control irrelevant peptide, peptide 5. As shown in Figure 3d, peptide 5, even at 100 nM, did not inhibit the interaction formed between biotin-labeled F11R and the immobilized M.Ab.F11, indicating that peptide 4D retains a high degree of specificity in blocking F11R-adhesive interactions.

In addition, in order to further understand the possible molecular basis underlying the recognition between peptide 4D and F11R, we performed molecular docking of peptide 4D into the proposed binding pocket of F11R. As shown in Figure

4, the four possible conformations adopted by peptide 4D docking into the binding pocket of F11R are presented. These conformations represent the best predicted structures based on the relative free energy of interaction of peptide 4D with its target protein F11R. The relative binding energy of interaction was determined with the built-in MMFF94 force-field of the docking software “Sculpt”. The best predicted conformations, presented in Panels a to d, were fitted within the steric active site of F11R, as predicted, from our earlier modeling of F11R.¹⁵

Real-time biomolecular and specific interactions between peptide 4D and, either the recombinant human F11R protein or the recombinant murine F11r protein, were measured with the surface plasmon resonance technology, using a BIAcore X apparatus equipped with a Sensor Chip CM-5. As shown in Figure 5a, peptide 4D (red colored tracing) exhibited a very high, specific response of its binding to the human F11R protein in comparison to the lack of binding shown by the control, nonbinding peptide, peptide 5 (blue tracing). Such results demonstrate a strong and specific binding between peptide 4D and the human F11R protein.

To examine whether the human peptide 4D interacts with the murine F11r protein, we utilized surface plasmon resonance to examine the binding of the human peptide 4D to the recombinant murine rmF11r protein. As shown in Figure 5b, the binding response was strong, and demonstrated that a specific interaction occurred between peptide 4D and the rmF11r molecule. Control experiments utilizing the irrelevant peptide demonstrated a complete lack of biomolecular interaction between the F11r protein and the control. Next, the data obtained by surface plasmon resonance were fitted to the mathematical Langmuir model for biomolecular interaction assuming a one-to-one interaction. The binding and rate constants characterizing the high degree of binding affinity of peptide 4D to the human recombinant protein rhF11R (Figure 5a) were calculated as follows: a dissociation constant, K_D of 17 nM; association constant, K_A of 5.90×10^7 1/M; and $k_d = 9.43 \times 10^{-6}$ 1/s, $k_a = 0.556 \times 10^3$ 1/Ms. Similar to human F11R, strong interactions were observed between peptide 4D and the recombinant murine protein F11r (Figure 5b): K_D of 33 nM; K_A of 3.20×10^7 1/M; and $k_d = 1.79 \times 10^{-5}$ 1/s, $k_a = 5.43 \times 10^3$ 1/Ms.

Experiments utilizing a solid-phase binding assay, demonstrating the homophilic binding between soluble, biotin-labeled F11R molecules and coated, immobilized F11R, were conducted to measure the ability of peptide 4D to interfere with this interaction. Figure 6a shows a dose-response curve of the binding of biotin-F11R to the immobilized F11R, with an IC_{50} value of ~ 200 nM and saturation occurring at ~ 900 nM. This homophilic interaction could be blocked, in a

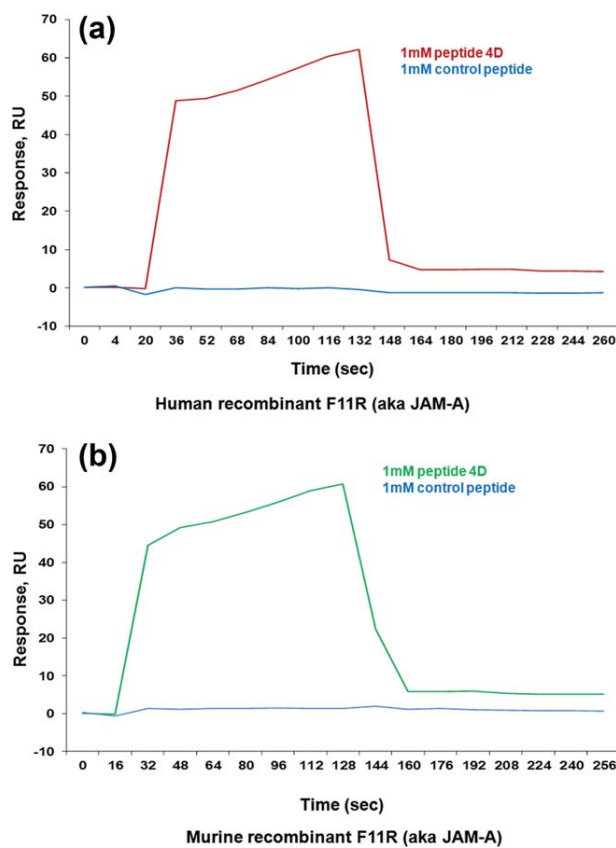


FIGURE 5 Specific interactions between peptide 4D and the human recombinant F11R and the murine recombinant F11r proteins, as probed by surface plasma resonance assay. Figure 5 (Panel a) demonstrates the specific binding between peptide 4D (1 mM) and the human recombinant F11R (F11R, aka rhJAM-A-Fc), as shown by the RED colored tracing. Control irrelevant peptide demonstrates the lack of binding to F11R (blue colored tracing). Fig.5 (Panel b) demonstrates a strong and specific interaction between peptide 4D (1 mM) and the murine recombinant F11r protein (GREEN color tracing). In comparison, a lack of binding with the recombinant murine F11r protein was observed when using an irrelevant, control peptide (blue colored tracing). Each tracing, as presented in both Panels a and b, is representative of tracings obtained in three separate experiments.

dose-dependent manner, by the addition of soluble, unlabeled F11R (IC_{50} 90 nM) (Figure 6b) and by peptide 4 (IC_{50} of 5 μ M) (Figure 6c). Similar concentrations of peptide 4D (Figure 6d) (in micromolar range) were utilized to block the interaction. The blockade indeed was specific, as irrelevant peptides did not produce such an inhibitory effect, even when used at concentrations of millimolar.

Another type of validation demonstrating the inhibitory effects of peptide 4D on the interaction between F11R molecules on separate F11R-expressing cells, was performed by examining the ability of peptide 4D to inhibit the adhesion of

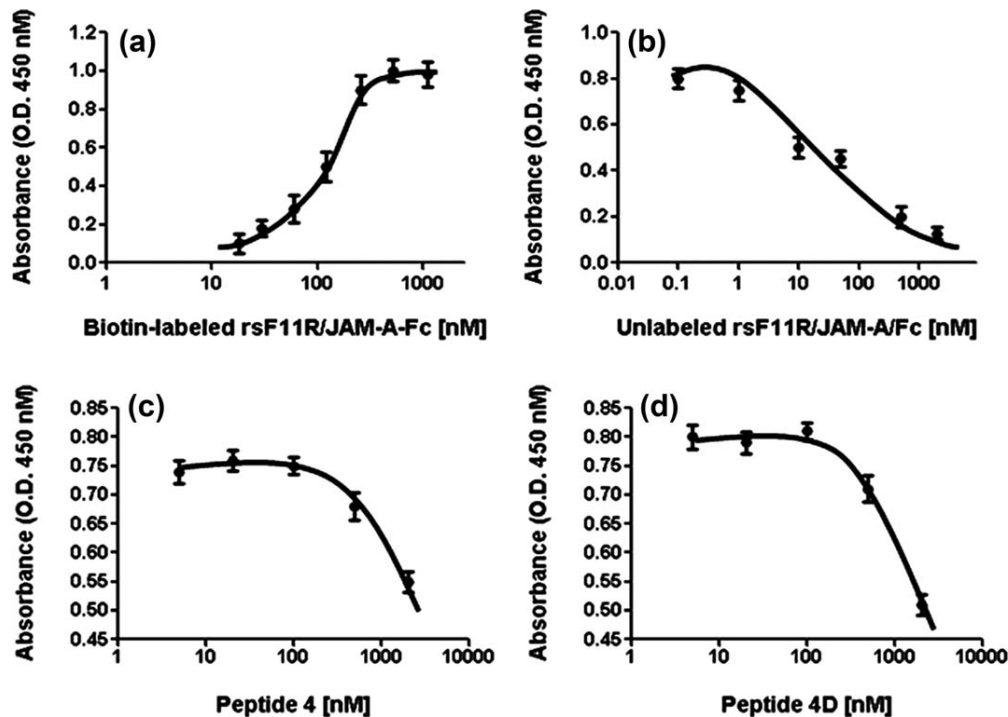


FIGURE 6 Inhibition of homophilic interaction between F11R molecules: blockade by peptide 4D using solid phase assay. Panel a) Homophilic interactions between F11R molecules - dose response. The binding of biotin-labeled F11R (recombinant soluble F11R, rsF11R aka JAM-A-Fc), performed at increasing concentrations, to unlabeled, immobilized F11R. Specific binding was determined by quantitating the amount of biotin-labeled F11R (recombinant soluble F11R, rsF11R/aka JAM-A-Fc) bound to immobilized, unlabeled F11R (recombinant soluble F11R, aka rsJAM-A/Fc). The specifically bound biotin-labeled F11R was quantitated as detailed in Methods. Panel b) Inhibition of the specific binding of biotin-labeled F11R (aka JAM-A-Fc) to immobilized F11R (aka F11R/JAM-A-Fc) by the addition of increasing concentrations of unlabeled rsF11R/JAM-A-Fc. Panel c) Inhibition of the specific binding of biotin-labeled F11R/JAM-A-Fc to immobilized F11R/JAM-A-Fc in the presence of increasing concentrations of peptide 4. Panel d) Inhibition of the specific binding of biotin-labeled F11R/JAM-A-Fc to immobilized F11R/JAM-A-Fc in the presence of increasing concentrations of the nonhydrolyzable peptide 4D. The fraction of bound ligand is given as the mean \pm SD of three separate experiments in each case.

human platelets to the inflamed endothelial cells. As shown in Figure 7 (panels a and b), F11R peptide 4D was capable of significantly blocking the binding of human platelets, nonactivated as well as collagen-activated platelets, to cytokine-inflamed endothelial cells (HUVEC treated simultaneously with the proinflammatory cytokines $\text{TNF}\alpha$ and $\text{INF}\gamma$). The histogram #1 in Figure 7 (panel a) depicts the specific adhesion of nonactivated platelets to cytokine-treated endothelial cells. However, in the presence of peptide 4D (as shown in histogram #2), we observed a significant inhibition (by 59%) of platelet adhesion to the inflamed endothelial cells due to the presence of peptide 4D (500 μM). Similarly, Figure 7 (panel b), histogram #1 depicts the specific adhesion of collagen-activated platelets to cytokine $\text{TNF}\alpha$ and $\text{INF}\gamma$ -inflamed

endothelial cells. However, in the presence of peptide 4D, such specific binding of activated platelets to inflamed endothelial cells was significantly inhibited (by 76%) due to the presence of 500 μM peptide 4D, as shown in histogram #2.

We observed that the effective inhibitory concentrations of peptide 4D in experiments involving the adhesion of platelets to cytokine-inflamed EC and platelet aggregation, were in the micromolar range, whereas the experiments involving solid phase binding were in the nanomolar range. These differences in order of magnitude can be attributed with great likelihood to the much higher degree of nonspecific binding that can be expected to occur in tests of living cell systems as compared to assays conducted with purified proteins.

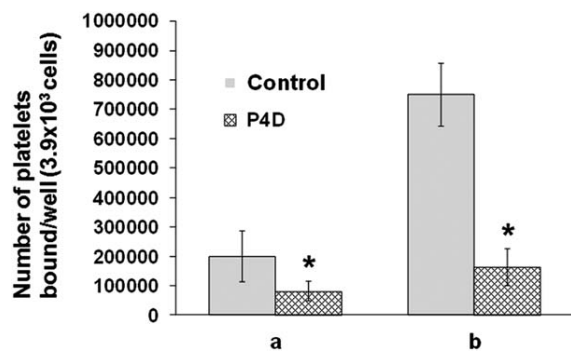


FIGURE 7 The adhesion of platelets to cytokine-inflamed endothelial cells: blockade by hydrolysis-resistant F11R peptide 4D. F11R peptide 4D blocked the adhesion of both activated platelets and non-activated platelets to cytokine TNF α and INF- γ -inflamed HUVEC. Panel a) Control histogram shows the adhesion of nonactivated platelets to cytokine-treated HUVEC in the absence of peptide 4D. P4D histogram shows significant blockade (by 59%) of the adhesion of platelets to inflamed HUVEC in the presence of peptide 4D (500 μ M). Panel b) Control histogram shows the adhesion of collagen-activated platelets to cytokine-treated HUVEC in the absence of peptide 4D. P4D histogram demonstrates that about 76% inhibition of the adhesion of activated platelets to the cytokine-inflamed HUVEC occurred in the presence of 500 μ M peptide 4D. The values represent the mean \pm SD of the number of platelets bound to ECs/per well obtained in three separate experiments in each condition in Panels a and b. The asterisk (*) indicates significance at a level of $P < 0.05$.

DISCUSSION

In previous reports,^{11,16} we have described the synthesis and testing of five peptides with sequences from five different regions of the external domain of the F11R protein. Of these five, two peptides named peptides 1 and 4, exhibited inhibition of the activity of F11R. Complete inhibition of M.Ab.F11-induced platelet aggregation occurred in the presence of \sim 50 μ M of either F11R peptide 1 or 4. In contrast, the addition of up to 500 μ M of peptides derived from other regions of the F11R sequence, named peptides 2 and 3, or peptide 5 used here as a control peptide, did not inhibit M.Ab.F11-induced platelet aggregation. Panels a, b and c in Figure 8 of the present report demonstrate a three-dimensional model of the external domain of the F11R molecule that provides the cause of these findings. The highlighted sequence of peptide 1 is localized within the N-terminus of the F11R protein, and the sequence of peptide 4 is confined to the 1st Ig-fold of F11R. Together, they create a putative “binding pocket” formed by two adjacent chains, one derived from the sequence of peptide 1 and the second from the sequence of peptide 4, located in an anti-parallel orientation, in close contact to each other, and exposed together at the outer surface of the cell membrane. We proposed that this exposed pocket operates as the adhesive contact-site, the active-site of the F11R protein.

Of the many molecular modelings used to identify the inter-cellular sites of association of F11R molecules between cells, the best-fit 3D-model is presented here in Figure 9, showing the area of interaction between two opposing F11R molecules. The model is constrained to the contact regions composed of the amino acid sequences within peptides 1 and 4. The dimerization interface, based on F11R crystal packing contacts, is depicted by the green and red colors. We hypothesized that potent candidates in the development of new therapeutic drugs could be designed based on the sequence and structure of this F11R dimerization interface. We initiated the experimental testing of this hypothesis by using peptides modified with D-amino acids.

Modifications involving D-amino acid substitutions are observed in peptides synthesized by animal and bacterial cells.^{22–27} The peptide bonds formed by D-amino acids are more resistant to proteases than those formed by their L-isomers as shown recently by X-Ray studies of human alpha-thrombin in complex with low μ M direct thrombin inhibitors (DTI) developed from D-Phe-Pro-D-Arg-P1'-CONH₂ tetrapeptides.¹⁸ The replacement of L-Arg with D-Arg within the scissile peptide bond L-Arg-P1', conferred 100% resistance to alpha-thrombin's hydrolysis of the corresponding DTI.¹⁸ These data strongly support the utilization of D-based peptides with enhanced stability to proteolysis by thrombin. Well-documented evidence demonstrates enhanced activity of thrombin during atherothrombosis.¹⁷ Therefore, in the study reported here we focused our investigation on the generation of those peptides which would demonstrate an increased lifetime at sites of atherosclerotic plaques with the development of D-analogs of F11R 4-L and 1L-peptides with stability to hydrolysis by thrombin.

The data from docking and modeling of the F11R peptide 4D within the proposed binding pocket of the F11R protein (see Figures 4, 8, 9), combined with the *in vitro* binding data utilizing solid phase binding assays (see Figures 3 and 6), as well as Surface Plasmon Resonance technology (see Figure 5), and the observed inhibition by peptide 4D of the aggregation and adhesion of platelets to the inflamed endothelium (see Figures 1, 2, 7), has allowed us to propose a model for the possible blockade of F11R interactions by peptide 4D—insertion of peptide 4D between the F11R molecules expressed on the surface of platelets and F11R molecules induced by cytokines to become exposed on the luminal surface of the inflamed endothelium (as depicted in Figure 10).

To-date, peptides prepared with amino acid sequences present as part of this protein-protein recognition interface, the active-site of F11R, have been demonstrated in our studies to act as inhibitors of platelet aggregation, as-well-as to inhibit the adhesion of platelets to inflamed EC.^{11,12,16,21}

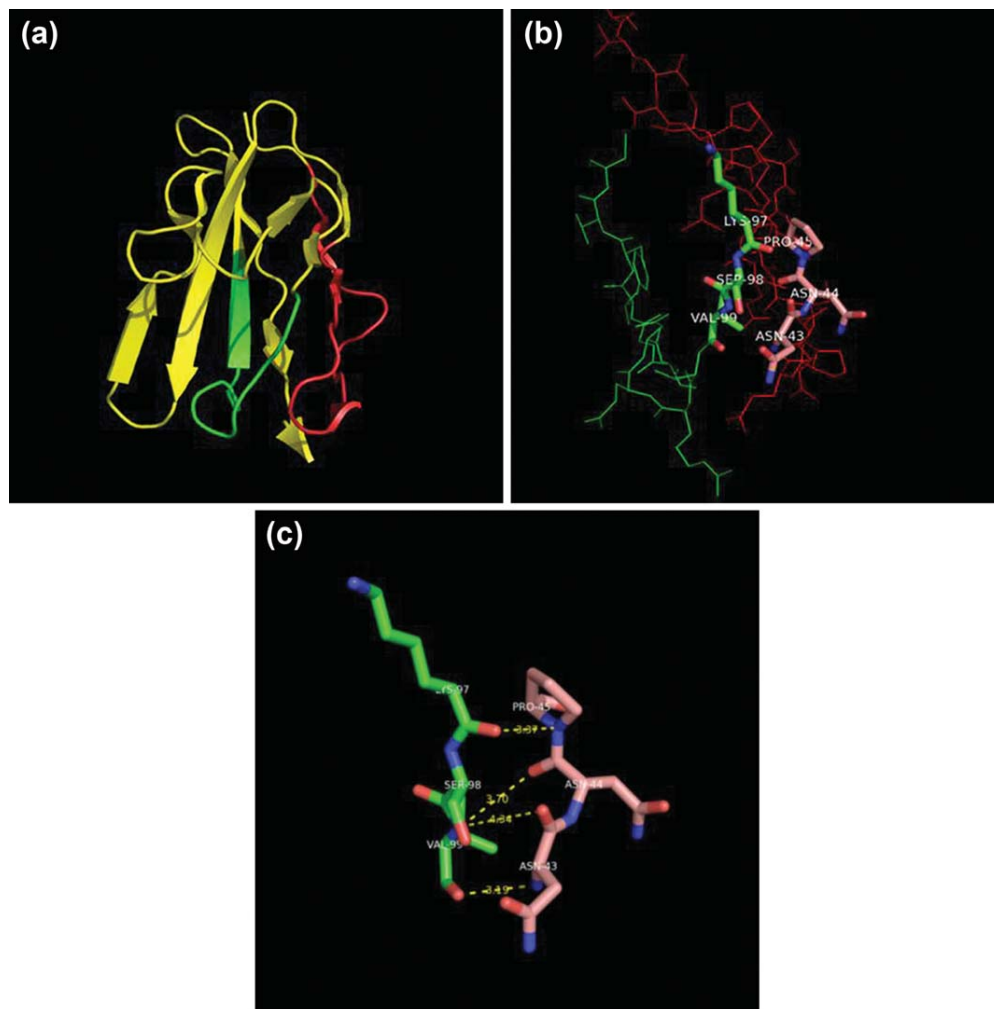


FIGURE 8 Three-dimensional modeling of the external domain of F11R: localization of amino acid sequences of inhibitory F11R peptides 1 and 4. Panel a) Ribbon model of F11R depicting the chain of the 23-amino acid sequence of peptide 1 (in red color) adjacent to the chain of 13-amino acids of peptide 4 (in green). The yellow color depicts the adjacent loops in the structure of F11R. Panel b) Ball and stick model of the amino acid sequence of peptide 1 (red color) and peptide 4 (green color) are shown in close contact on the membrane surface, displaying both the 3D position of the atoms and the bonds between them. The closest amino acids on the adjacent loops of F11R are shown by the dark green color of amino acids lys 97, ser 98 and val 99 within peptide 4, and by the pink color of amino acids asn 43, asn 44 and pro 45 of peptide 1. (Residues from peptides 1 and 4 that are within close contact to each other are available on the membrane surface as potential contact sites (other residues are at least partially buried). Panel c) An enlarged depiction showing the distances between atoms of peptides 1 (pink) and peptide 4 (green).

These results have allowed us to select and modify the lead peptide which we currently use in-vivo, in studies of the inhibition of atherosclerotic-plaque formation in an animal model of atherosclerosis. The results presented here, together with our initial positive results in vivo, clearly demonstrate that peptide 4D should be tested NOW in human patients as

a therapeutic agent for the prevention and regression of atherosclerotic plaque formation.

The crystal structure of the active-site of F11R also provides most useful guidelines for future developments. First, it shows that the sequence of peptide 4 is located on the external membrane surface and thus a single peptide may inhibit the

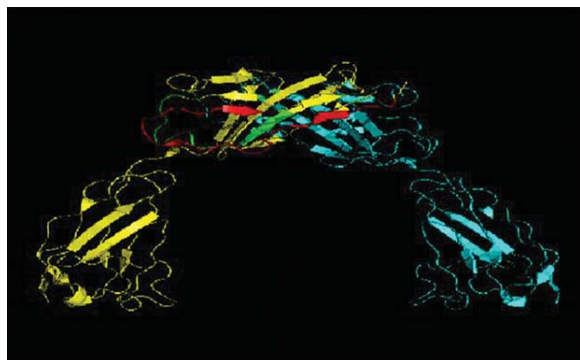


FIGURE 9 Adhesion of cells by homophilic binding of two F11R molecules based on crystal packing contacts. F11R molecules, expressed on the membrane surface of cells, bind to each other across the intercellular space, potentially via contacts within regions of amino acid sequences present in peptides 1 and 4 (green, red colors, respectively). Potent new drugs can be designed based on the sequence and structure of this region.

homodimeric F11R-interactions by mimicking and binding to this sites. Second, the sequence of chains within the crystal structure indicates that only a few amino acids of each peptide are exposed on the binding and dimerization interface of the F11R molecule. Therefore, peptides with much shorter sequences may be sufficient for inhibiting F11R–F11R homophilic interactions. Furthermore, the combined steric and sequence data in the crystal model of the active-site provide the information for the design and synthesis of nonpeptide, so-called peptidomimetic inhibitors of the patho-physiologic action of F11R. These can be more suitable than modified peptides for daily, long-term treatment of patients suffering from cardiovas-

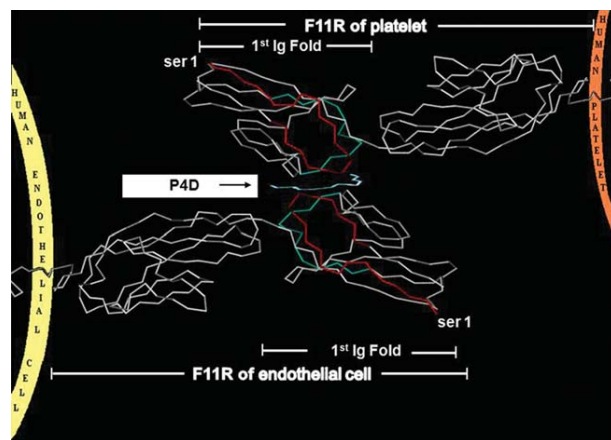


FIGURE 10 A molecular model demonstrating the interaction between an F11R molecule, constitutively expressed on the platelet membrane surface, and an F11R molecule expressed on the luminal surface of a cytokine-inflamed endothelial cells: the insert designated P4D demonstrates the blockage of F11R interactions by peptide 4D.

cular disorders. Several statins that are currently used as drugs of choice in these patients, target cholesterol and lipid metabolism. The specific biochemical target of action of F11R-antagonists is very different: i.e., the adhesion of platelets (and possibly other circulating cells) to an inflamed, atherogenic endothelium. We propose that a combined administration of BOTH types of drugs together, may provide an additive, or even synergistic therapeutic advantage for the prevention and treatment of thrombosis, atherosclerosis, heart-attacks, and stroke.

REFERENCES

- Kornecki, E.; Walkowiak, B.; Naik, U. P.; Ehrlich, Y. H. *J Biol Chem* 1990, 265, 10042–10048.
- Naik, U. P.; Ehrlich, Y. H.; Kornecki, E. *Biochem J* 1995, 311, 155–162.
- Sobocka, M. B.; Sobocki, T.; Banerjee, P.; Weiss, C.; Rushbrook, J. I.; Norin, A. J.; Hartwig, J.; Salifu, M. O.; Markell, M. S.; Babinska, A.; Ehrlich, Y. H.; Kornecki, E. *Blood* 2000, 95, 2600–2609.
- Sobocki, T.; Sobocka, M. B.; Babinska, A.; Ehrlich, Y. H.; Banerjee, P.; Kornecki, E. *Gene* 2006, 17, 128–144.
- Martin-Padura, I.; Lostaglio, S.; Schneemann, M.; Williams, L.; Romano, M.; Fruscella, P.; Panzeri, C.; Stoppacciaro, A.; Ruco, L.; Villa, A.; Simmons, D.; Dejana, E. *J Cell Biol* 1998, 142, 117–127.
- Ostermann, G.; Fraemohs, L.; Baltus, T.; Schober, A.; Lietz, M.; Zernecke, A.; Liehn, E. A.; Weber, C. *Arterioscler Thromb Vasc Biol* 2005, 25, 729–735.
- Gawaz, M.; Langer, H.; May, A. E. *J Clin Invest* 2005, 115, 3378–3384.
- Langer, H. F.; Gawaz, M. *Thromb Haemost* 2008, 99, 480–486.
- Theilmeyer, G.; Michiels, C.; Spaepen, E.; Vreys, I.; Collen, D.; Vermynen, J.; Hoylaerts, M. F. *Blood* 2002, 99, 4486–4493.
- Massberg, S.; Brand, K.; Grüner, S.; Page, S.; Müller, E.; Müller, I.; Bergmeier, W.; Richter, T.; Lorenz, M.; Konrad, I.; Nieswandt, B.; Gawaz, M. A. *J Exp Med* 2002, 196, 887–896.
- Babinska, A.; Kedeas, M. M.; Athar, H.; Batuman, O.; Ehrlich, Y. H.; Hussain, M. M.; Kornecki, E. *Thromb Haemost* 2002, 88, 843–850.
- Babinska, A.; Azari, B. M.; Salifu, M. O.; Liu, R.; Jiang, X. C.; Sobocka, M. B.; Boo, D.; Khoury, G. A.; Deitch, J. S.; Marmur, J. D.; Ehrlich, Y. H.; Kornecki, E. *Thromb Haemost* 2007, 97, 272–281.
- Azari, B. M.; Marmur, J. D.; Salifu, M. O.; Cavusoglu, E.; Ehrlich, Y. H.; Kornecki, E.; Babinska, A. *Atherosclerosis* 2010, 212, 197–205.
- Azari, B. M.; Marmur, J. D.; Salifu, M. O.; Ehrlich, Y. H.; Kornecki, E.; Babinska, A. *J Translational Med* 2011, 9, 98.
- Prota, A. E.; Campbell, J. A.; Schelling, P.; Forrest, J. C.; Watson, M. J.; Peters, T. R.; Aurrand-Lions, M.; Imhof, B. A.; Dermody, T. S.; Stehle, T. *Proc Nat Acad Sci USA* 2003, 100, 5366–5371.
- Babinska, A.; Kedeas, M. H.; Athar, H.; Sobocki, T.; Sobocka, M. B.; Ahmed, T.; Ehrlich, Y. H.; Hussain, M. M.; Kornecki, E. *Thromb Haemost* 2002, 87, 712–721.

17. Lee, I. O.; Kratz, M. T.; Schirmer, S. H.; Baumhäkel, M.; Böhm, M. *J Pharmacol Exp Ther* 2012, 343, 253–257.
18. Figueiredo, A. C.; Clement, C. C.; Zakia, S.; Gingold, J.; Philipp, M.; Pereira, P. J. *PLoS One* 2012, 7, e34354.
19. Heger, M.; Salles, I. L.; van Vuure, W.; Hamelers, I. H.; de Kroon, A. I.; Deckmyn, H.; Beek, J. F. *Microvascular Res* 2009, 78, 57–66.
20. Braut-Boucher, F.; Pichon, J.; Rat, P.; Adolphe, M.; Aubery, M.; Font, J. *J Immunol Methods* 1995, 178, 41–51.
21. Kedees, M. H.; Babinska, A.; Swiatkowska, M.; Deitch, J.; Ehrlich, Y. H.; Kornecki, E. *Platelets* 2005, 16, 99–110.
22. Sela, M.; Zisman, E. *FASEB J* 1997, 11, 449–456.
23. Che, Y.; Marshall, G. R. *J Med Chem* 2006, 49, 111–124.
24. Luo, Z.; Yue, Y.; Zhang, Y.; Yuan, X.; Gong, J.; Wang, L.; He, B.; Liu, Z.; Sun, Y.; Liu, J.; Hu, M.; Zheng, J. *Biomaterials* 2013, 34, 4902–4913.
25. Van Regenmortel, M. H.; Muller, S. *Curr Opin Biotechnol* 1998, 9, 377–382.
26. Wolosker, H.; Dumin, E.; Balan, L.; Foltyn, V. N. *FEBS J* 2008, 275, 3514–3526.
27. Akita, H.; Suzuki, H.; Doi, K.; Ohshima, T. *Appl Microbiol Biotechnol* 2014, 98, 1135–1143.